Chinese Chemical Letters 35 (2024) 109697

Contents lists available at ScienceDirect

Chinese Chemical Letters

journal homepage: www.elsevier.com/locate/cclet

$CaCO_3$-coated hollow mesoporous silica nanoparticles for pH-responsive fungicides release

Jiaxu Wang[a,b,1], Jinxie Zhang[a,1], Xiuping Wang[b,1], Jingying Wang[a,b], Lina Chen[b], Jiahui Cao[a], Wei Cao[a], Siyu Liang[c], Ping Luan[d], Ke Zheng[e], Xiao-Kun Ouyang[f], Li Gao[g], Xiaowen Ou[a], Fan Zhang[a,*], Meitong Ou[a,*], Lin Mei[a,*]

[a] State Key Laboratory of Advanced Medical Materials and Devices, Tianjin Key Laboratory of Biomedical Materials, Key Laboratory of Biomaterials and Nanotechnology for Cancer Immunotherapy, Institute of Biomedical Engineering, Chinese Academy of Medical Sciences and Peking Union Medical College, Tianjin 300192, China
[b] Hebei Key Laboratory of Crop Stress Biology, College of Agronomy and Biotechnology, Hebei Normal University of Science and Technology, Qinhuangdao 066000, China
[c] University of Edinburgh, Old College, South Bridge, Edinburgh EH89YL, Scotland, United Kingdom
[d] School of Basic Medical Sciences, Shenzhen University, Shenzhen 518060, China
[e] School of Materials Science and Engineering, Dongguan University of Technology, Dongguan 523808, China
[f] School of Food and Pharmacy, Zhejiang Ocean University, Zhoushan 316022, China
[g] The Second Affiliated Hospital of Guilin Medical College, Guilin 541199, China

ARTICLE INFO

Article history:
Received 26 December 2023
Revised 23 February 2024
Accepted 25 February 2024
Available online 2 March 2024

Keywords:
Nanopesticide
pH-responsive
Controlled release
Mesoporous silica nanoparticles
Sclerotinia sclerotiorum
Dimethachlon

ABSTRACT

The utilization of fungicides in plants is very low, emphasizing the need to improve their utilization rates. In this study, the fungicide dimethachlon (Dim) was encapsulated within hollow mesoporous silica (HMSNs), and a coating was formed on the HMSNs surface through the reaction of Na_2CO_3 and $CaCl_2$, resulting in a pH-responsive delivery system named D/H@$CaCO_3$, proven valuable in preventing sclerotinia diseases in romaine lettuce. When disease-infested romaine lettuce was treated with D/H@$CaCO_3$, it degraded in the acidic microenvironment of *Sclerotinia sclerotiorum* (*S. sclerotiorum*), allowing for the pH-responsive release of Dim and effectively killing *S. sclerotiorum*. Moreover, the degraded $CaCO_3$ coating releases CO_2, which enhances the photosynthetic pigment contents, such as chlorophyll a, chlorophyll b, and carotenoids, in turn promoting plant growth. D/H@$CaCO_3$ is biologically safe for plants and is environmentally friendly, as confirmed by assessments involving zebrafish and earthworms. Given their antifungal capabilities, the controlled release of fungicides offers potential for plant protection.

Fungicides play an indispensable role in modern agriculture, serving as the primary means of protecting crops from pests and plant pathogens, thereby increasing yield [1–3]. However, traditional fungicides are prone to evaporation and photolysis, significantly reducing effectiveness against organisms. According to estimates by the Food and Agriculture Organization, using fungicides can recover 30%–40% of the total global crop output [4], however, fungicide residues can subsequently harm both plants and aquatic life [5,6]. Reducing fungicide losses, ensuring efficient fungicide delivery, and enabling on-demand release are crucial for improving the efficiency of fungicide usage and minimizing environmental pollution.

Sclerotinia sclerotiorum (*S. sclerotiorum*) is one of the most destructive plant pathogens that infects romaine lettuce and can lead to substantial production losses. Upon colonization of the romaine lettuce surface, *S. sclerotiorum* produces extracellular enzymes that foster an acidic microenvironment [7–9], which damages the plant cell walls and contributes to a marked reduction in romaine lettuce yield. Dimethachlon (Dim) is a common fungicide that is remarkably effective at inhibiting *S. sclerotiorum*. However, their effectiveness, utilization, and persistence are significant because they decompose in the presence of acid-base and sunlight [10]. Therefore, there is an urgent need to design a delivery system that extends the duration of fungicide use, enhances the utilization rate, ensures biosafety, and remains environmentally friendly.

* Corresponding authors.
E-mail addresses: zhangfan@bme.pumc.edu.cn (F. Zhang), oumt@bme.pumc.edu.cn (M. Ou), meilin@bme.pumc.edu.cn (L. Mei).
[1] These authors contributed equally to this work.

https://doi.org/10.1016/j.cclet.2024.109697
1001-8417/

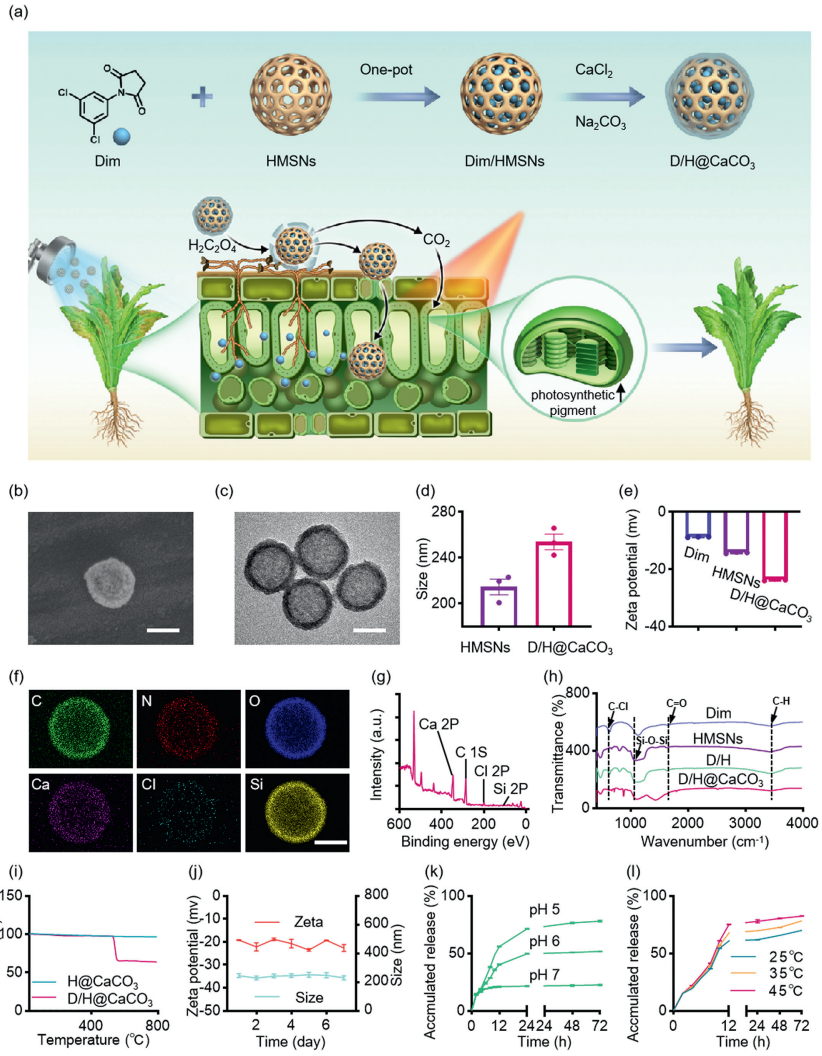

Fig. 1. (a) Schematic illustration for preparing D/H@$CaCO_3$ and the mechanism of enhanced *S. sclerotiorum* inhibition and plant photosynthesis. The preparation procedure of D/H@$CaCO_3$. D/H@$CaCO_3$ responds to the acidic microenvironment of *S. sclerotiorum* to release Dim and CO_2. This enhances the inhibitory effect of Dim on *S. sclerotiorum*, and the CO_2 generated by $CaCO_3$ further promotes photosynthesis in romaine lettuces. (b) SEM and (c) TEM of D/H@$CaCO_3$. Scale bar: 100 nm. (d) Hydrodynamic diameters of HMSNs and D/H@$CaCO_3$. (e) Zeta potentials of Dim, HMSNs, and D/H@$CaCO_3$. (f) EDS mapping of D/H@$CaCO_3$. Scale bar: 100 nm. (g) XPS image of D/H@$CaCO_3$. (h) FTIR spectra of Dim, HMSNs, D/H and D/H@$CaCO_3$. (i) TGA curves of H@$CaCO_3$ and D/H@$CaCO_3$. (j) Zeta potential and hydrodynamic diameters changes of D/H@$CaCO_3$ at 0 °C for 7 days. (k) Release behavior of D/H@$CaCO_3$ at pH 5, 6, and 7 (35 °C) and (l) temperatures at 25, 35, 45 °C (pH 5). Data are presented as means ± SEM (n = 3).

Hollow mesoporous silica nanoparticles (HMSNs) have been widely utilized as a delivery system for both medicines and fungicides owing to their advantageous properties, such as large surface area, tunable size, high stability, and biocompatibility [11–16]. Wang *et al.* developed an oxidation-resistant ferrous foliar fertilizer delivery system that utilizes hollow silicon as a carrier for ferrous foliar. This not only enhances the adhesion efficiency of the foliar but also boosts its antioxidant capacity, effectively addressing iron deficiency in crops, and thus significantly elevating crop yield [17]. Similarly, Ding *et al.* a mesoporous silica nano-carrier pesticide delivery system loaded with acetamiprid was constructed, which improved the control effect of aphids and reduced pesticide residues [18]. Leveraging HMSNs for pesticide delivery can bolster formulation stability, curtail soil leaching, and prolong effectiveness while minimizing environmental toxicity [19–24].

In this study, we encapsulated Dim in HMSNs using a one-pot method, followed by a $CaCO_3$ film coating on the surface of the HMSNs through the reaction of Na_2CO_3 and $CaCl_2$, creating a Dim delivery system called D/H@$CaCO_3$ (Fig. 1a). The $CaCO_3$ film exhibited pH-responsive release properties and acted as a regulator of Dim release. When romaine lettuce leaves were contaminated with *S. sclerotiorum* and treated with D/H@$CaCO_3$, the $CaCO_3$ film acted as a "gatekeeper", facilitating the controlled degradation of D/H@$CaCO_3$ in the acidic microenvironment of *S. sclerotiorum*-infested romaine lettuce and ensuring the pH-responsive release of Dim from the HMSNs. This effectively enhances the antifungal effect, thus curtailing the growth of *S. sclerotiorum*. Simultaneously, the decomposed $CaCO_3$ produces CO_2, which aids plant photosynthesis and benefits plant growth. Furthermore, D/H@$CaCO_3$ is environmentally safe and does not hamper the growth of romaine lettuce because the main component of D/H@$CaCO_3$ is HMSNs.

Dim was loaded into the HMSNs, followed by the coating of a film of $CaCO_3$ onto the surface *via* the reaction of Na_2CO_3 and $CaCl_2$. This resulted in the formation of pH-responsive fungicide nanoparticles (D/H@$CaCO_3$) for delivery to romaine lettuce. The morphology of D/H@$CaCO_3$ was observed by scanning electron microscopy (SEM) and transmission electron microscopy (TEM), D/H@$CaCO_3$ was spherical with a rough surface (Fig. 1b) and a visible coating $CaCO_3$ layer on its surface (Fig. 1c). We also investigated the particle size and potential of D/H@$CaCO_3$. The size of D/H@$CaCO_3$ was approximately 255 nm, about 40 nm larger than HMSNs (Fig. 1d). The zeta potential of Dim, HMSNs,

and D/H@$CaCO_3$ was −8.72, −14.20, and −23.69 mV, respectively (Fig. 1e). The energy dispersive spectrometer (EDS) mapping analysis revealed that D/H@$CaCO_3$ primarily contained Cl, N, Si, Ca, C, and O. Ca and C were mainly attributed to $CaCO_3$, whereas Si originated from SiO_2, Cl and N originated from Dim (Fig. 1f). The X-ray photoelectron (XPS) analysis of D/H@$CaCO_3$ (Fig. 1g) showed a pronounced Si 2p peak at 103.22 eV, corresponding to the primary element of the HMSNs (Fig. S1a in Supporting information). Distinct Cl 2p and C 1s peaks were observed at 198.74 and 285.38 eV, respectively, indicating the presence of Dim as the main component in D/H@$CaCO_3$ (Figs. S1b and c in Supporting information). Additionally, a well-defined Ca 2p peak at 345.94 eV confirms the presence of coated $CaCO_3$ (Fig. S1d in Supporting information), validating the structural composition of D/H@$CaCO_3$. The functional groups in D/H@$CaCO_3$ were characterized through Fourier transform infrared spectroscopy (FTIR) (Fig. 1h), showing characteristic peaks associated with Si-O-Si bonds at 1094.89 cm^{-1} in the HMSNs group. As for the Dim group, distinctive absorption peaks corresponded to C–Cl bond at 616.102 cm^{-1}, along with peaks at 1632.282 cm^{-1} for C=O. The absorption peak at 3411.178 cm^{-1} was attributed to the stretching vibration of the =C–H bond. The D/H@$CaCO_3$ spectra exhibited peaks originating from both Dim and HMSNs. The Dim loading efficiency of D/H@$CaCO_3$ was determined by thermogravimetric analysis (TGA) (Fig. 1i). The HMSNs exhibited a final mass loss rate of 3.31%, attributed to water evaporation and decomposition of organic functional groups. In comparison, D/H@$CaCO_3$ showed a higher final mass loss rate of 36.41%, which indicated the loss of both organic matter and Dim, and the Dim loading rate was calculated to be 33.1%.

The stability of D/H@$CaCO_3$ was assessed by monitoring the variations in zeta potential and particle size at 0 °C and 54 °C [25]. At 0 °C, the potential remained stable at approximately −21 mV for 7 days, and the particle size distributed around 241 nm (Fig. 1j). Similarly, at 54 °C, the potential was stable at around −24 mV for 14 days, and the particle size distribution was around 238 nm (Fig. S2 in Supporting information). These results demonstrate the optimal stability of D/H@$CaCO_3$.

To effectively control the release of fungicides into the acidic microenvironment of *S. sclerotiorum*, a pH-responsive system that releases Dim under acidic conditions is crucial. The designed $CaCO_3$ coating on the D/H surface degraded under acidic conditions. We tested the pH-responsive release efficacy of D/H@$CaCO_3$ at pH 5, 6, and 7 and temperatures of 25, 35, and 45 °C. As depicted in Fig. 1k, the cumulative release rates at 35 °C over a 48 h period were 76.48%, 50.76%, and 22.08% at pH 5, 6, and 7, respectively. This indicates that, in a weakly acidic microenvironment, D/H@$CaCO_3$ can respond to degradation, enabling the responsive release of Dim. Furthermore, we studied release rates at pH 5 and 25, 35, and 45 °C, which were 65.68%, 72.60%, and 80.38% at 48 h, respectively, suggesting that higher temperatures facilitate Dim release (Fig. 1l). Additionally, we utilized zero-, first-, and higher-order release kinetic models to analyze the release kinetics of D/H@$CaCO_3$ (Figs. S3 and S4 in Supporting information).

We have previously demonstrated that D/H@$CaCO_3$ is degraded in the acidic microenvironment of *S. sclerotiorum*. Moreover, degraded $CaCO_3$ can generate CO_2 under acidic conditions. We used a bromothymol blue solution to test the generation of CO_2 using D/H@$CaCO_3$ under acidic conditions. By adding an oxalic acid solution to D/H@$CaCO_3$, we simulated the microenvironment of *S. sclerotiorum*, the degradation of D/H@$CaCO_3$ caused the CO_2 release, progressively changing the color of bromothymol blue from blue to green and ultimately to yellow. As shown in Fig. 2a, when the D/H@$CaCO_3$ concentration ranged from 0 to 1 mg/mL, the indicator changed from blue to yellow. This color shift suggests that as the concentration of D/H@$CaCO_3$ increased, the CO_2 production increased. We further investigated whether the CO_2 produced by D/H@$CaCO_3$ in the acidic microenvironment of *S. sclerotiorum* could enhance photosynthetic pigments in plants (Fig. 2b). In Fig. 2c different concentrations of D/H@$CaCO_3$ were used to treat romaine lettuce in the acidic microenvironment.

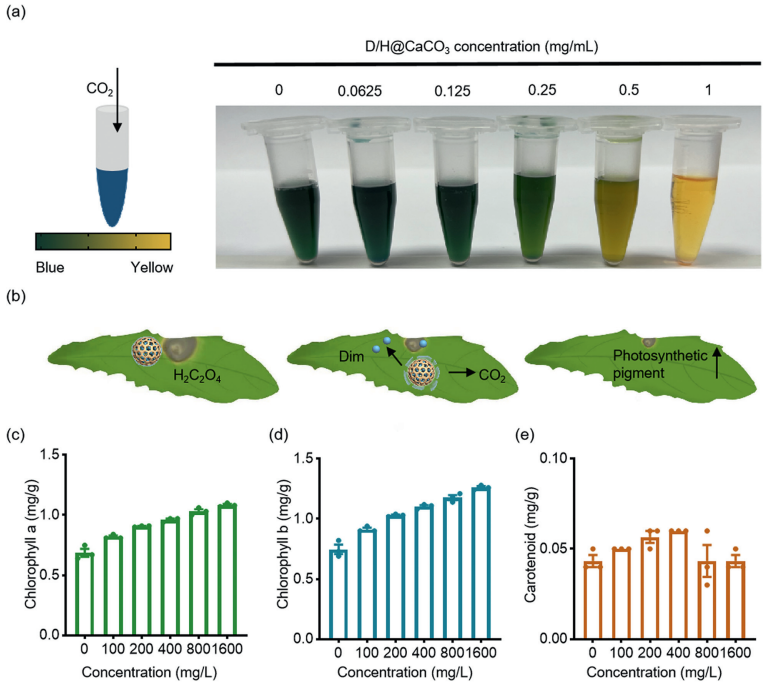

Fig. 2. (a) Color changes in bromothymol blue indicator after treatment with CO_2 generated by different concentrations D/H@$CaCO_3$. (b) Schematic illustration of D/H@$CaCO_3$ promoting plant photosynthesis. $CaCO_3$ coated on D/H@$CaCO_3$ degrading and generating CO_2 in the acidic microenvironment of *S. sclerotiorum*, which could be beneficial for plant photosynthesis and plant growth. (c) Chlorophyll a, (d) chlorophyll b, and (e) carotenoids levels in the leaves treated with different concentrations of D/H@$CaCO_3$. Data are presented as means ± SEM (n = 3).

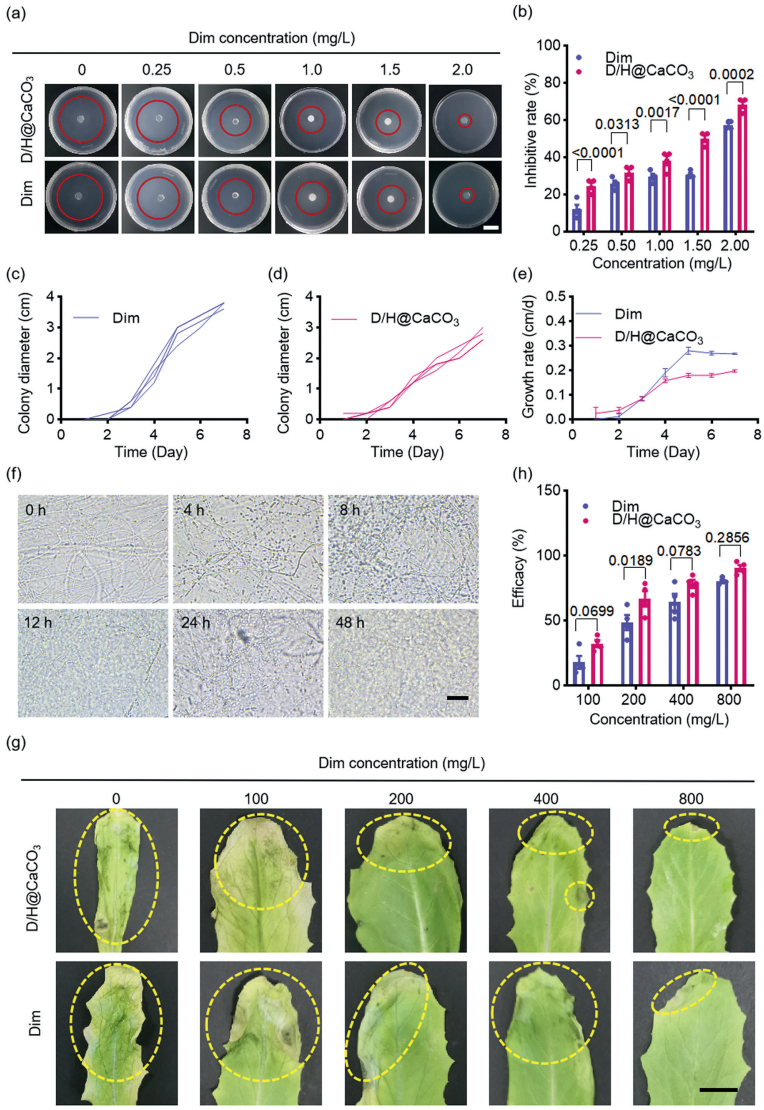

Fig. 3. (a) Photos of *S. Sclerotiorum* colony on the 7th day after administration of Dim or D/H@$CaCO_3$. A red circle represents the fungal colony (scale bar: 2 cm). (b) The quantitative analysis of inhibition rate of Dim or D/H@$CaCO_3$ against *S. sclerotiorum*. (c, d) The colony diameter was measured at 0, 1, 2, 3, 4, 5, 6 and 7 days after treatment with Dim or D/H@$CaCO_3$ at an effective Dim concentration of 1.5 mg/L. (e) The growth rate of Dim and D/H@$CaCO_3$ against *S. sclerotiorum* at an effective Dim concentration of 1.5 mg/L. (f) Microscopic images of hyphae at 0, 4, 8, 12, 24 and 48 h after D/H@$CaCO_3$ treatment. Scale bar: 50 μm. (g) Photos of *S. sclerotiorum*-infested romaine leaves on the 7th day after being treated with different concentrations of D/H@$CaCO_3$ or Dim. Scale bar: 1 cm. (h) Control efficacy of Dim and D/H@$CaCO_3$ in controlling Sclerotinia disease. Data in (b) and (h) are compared by one-way ANOVA. $^{*}P < 0.05$, $^{**}P < 0.01$, $^{***}P < 0.001$. Data are presented as means ± SEM ($n = 4$).

When the D/H@$CaCO_3$ concentrations were 0, 100, 200, 400, 800, and 1600 mg/L, the chlorophyll a content was 0.69, 0.82, 0.91, 0.96, 1.03, and 1.09 mg/g, respectively. The chlorophyll b content also increased with increasing D/H@$CaCO_3$ concentration (Fig. 2d). When the D/H@$CaCO_3$ concentration reached 200 mg/L, its carotenoid content surged to 0.059 mg/g, as evident in Fig. 2e. This shows that the CO_2 released from D/H@$CaCO_3$ in the *S. sclerotiorum* microenvironment promotes photosynthesis, benefiting plant growth. When the D/H@$CaCO_3$ concentration exceeded 400 mg/L, it could generate excess CO_2 for photosynthesis over the long term. This elevated CO_2 treatment could lead to more membrane damage due to reactive oxygen species, thus resulting in the loss of photosynthetic pigments and lowering of the carotenoid accumulation [26,27].

To evaluate the antifungal activity of D/H@$CaCO_3$ against *S. sclerotiorum*, the fungus was exposed to various concentrations of D/H@$CaCO_3$. As depicted in Fig. 3a, after a 7-day exposure to D/H@$CaCO_3$, the fungal colony size decreased with increasing D/H@$CaCO_3$ concentration, indicating enhanced suppression of *S. sclerotiorum*. A quantitative analysis of the inhibition rate in Fig. 3a was shown in Fig. 3b. At Dim concentrations of 0.25, 0.50, 1.00, 1.50, and 2.00 mg/L, D/H@$CaCO_3$ displayed inhibition rates of 24.55%, 31.82%, 38.18%, 50.00%, and 68.18% respectively. In contrast, Dim alone resulted in inhibition rates of 12.04%, 25.93%, 29.63%, 30.56%, and 57.41% (Fig. 3b). Figs. 3c and d reveal that on the second day, the Dim-treated group exhibited a smaller average diameter of the inhibition zone than the D/H@$CaCO_3$ group at an effective Dim concentration of 1.5 mg/L. On the third day, the Dim group displayed a *S. sclerotiorum* growth rate of 0.08 cm/d, whereas that of the D/H@$CaCO_3$ group was 0.08 cm/d. By the seventh day, these rates were 0.27 cm/d for the Dim group and 0.20 cm/d for D/H@$CaCO_3$ group (Fig. 3e). For a more detailed evaluation, we further utilized an effective Dim concentration of 0.25, 0.50, 1.00 and 2.00 mg/L to gage the *S. sclerotiorum* growth rate with D/H@$CaCO_3$ group at intervals of 1, 2, 3, 4, 5, 6 and 7 days (Figs. S5a–d in Supporting information). These findings suggest that D/H@$CaCO_3$ maintains its antifungal activity longer than Dim alone. This enhancement can be attributed to D/H@$CaCO_3$ facilitating the controlled release of Dim, with $CaCO_3$ serving as a protective "gate-

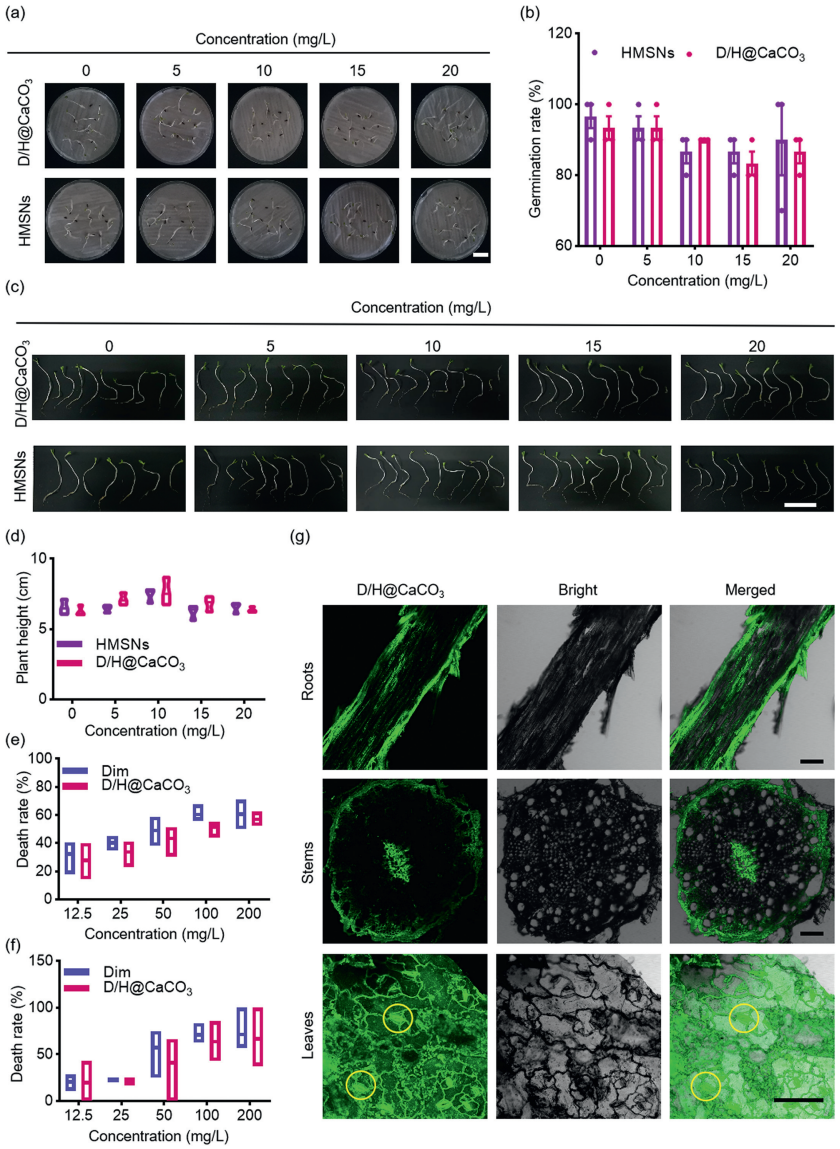

Fig. 4. (a) Photographs (scale bar: 20 mm) and (b) germination rate of seeds after 5 days of treatment with HMSNs or D/H@$CaCO_3$ at different concentrations. (c) Photographs (scale bar: 5 cm) and (d) plant height after 12 days of treatment with HMSNs or D/H@$CaCO_3$ at different concentrations. The death rate of (e) earthworms and (f) zebrafish after 48 h of treatment with Dim or D/H@$CaCO_3$. (g) Confocal images of romaine roots, stems, and leaves after being treated with FITC-stained D/H@$CaCO_3$. Green fluorescence represents FITC-stained D/H@$CaCO_3$. Scale bar: 100 μm. Data are presented as means ± SEM ($n = 3$).

keeper", triggering the release of Dim in acidic microenvironments and enhancing its inhibition against fungi. Upon administering D/H@$CaCO_3$ to *S. sclerotiorum*, retardation of hyphal growth was observed. The hyphae showed progressive fragmentation over 0, 4, 8, 12, 24, and 48 h (Fig. 3f). However, pronounced hyphal death was observed at the 12 h mark. In addition, we examined the effects of D/H@$CaCO_3$ on the fungicidal activity on romaine lettuce. Romaine lettuce leaves were inoculated with *S. sclerotiorum* and treated with different concentrations of D/H@$CaCO_3$ and Dim. Seven days later, a distinct reduction in the fungicidal plaque size was observed as the solution concentration increased, and the leaves appeared healthy (Fig. 3g). According to our quantitative analysis, at Dim concentrations of 100, 200, 400, and 800 mg/L, the control efficiencies of D/H@$CaCO_3$ reached 32.42%, 66.88%, 78.43%, and 90.44%, respectively, while the efficiencies of the Dim group in the precaution and control groups were 17.97%, 48.65%, 64.31%, and 80.38%, respectively (Fig. 3h). Compared with Dim alone, D/H@$CaCO_3$ could protect Dim from decomposition in the presence of sunlight, which enhanced the utilization of fungicides. Furthermore, the $CaCO_3$ film could release Dim in the acidic microenvironment of *S. sclerotiorum*-infested romaine lettuce, which provided better antifungal effectiveness and persistence of Dim for the responsive release. Therefore, D/H@$CaCO_3$ showed more effective in inhibiting on *S. sclerotiorum* than that of Dim alone.

We assessed the safety of the D/H@$CaCO_3$. Figs. 4a and b show that plants treated with 20 mg/L D/H@$CaCO_3$ still exhibited a germination rate greater than 85%. When applying concentrations of D/H@$CaCO_3$ at 0, 5, 10, 15 and 20 mg/L to plants, the recorded plant heights were 6.27, 7.12, 7.65, 6.82, and 6.37 cm, respectively (Figs. 4c and d). This demonstrates that D/H@$CaCO_3$ did not adversely affect plant height. Moreover, after treatment with HMSNs or D/H@$CaCO_3$, there was no discernible difference in the germination rate or rapeseed biomass, further validating the negligible effect of D/H@$CaCO_3$ on seedling growth. The infiltration of Dim residues into soil and water poses a significant danger to soil organisms and aquatic ecosystems. Earthworms and zebrafish were evaluated to assess the environmental safety of D/H@$CaCO_3$. Figs. 4e and f show the mortality rates of earthworms

and zebrafish exposed to D/H@$CaCO_3$. At concentrations of 12.5, 25, 50, 100, or 200 mg/L, the average mortality rates were 27.77%, 33.80%, 43.37%, 51.34%, or 56.89% for earthworms, and 19.84%, 22.22%, 41.27%, 63.69%, or 66.67% for zebrafish. The lethal concentration 50% (LC_{50}) values of the D/H@$CaCO_3$ group surpassed those of the Dim group for both organisms. For earthworms, it was 51.83 mg/L in the Dim group (95% confidence interval: 26.17 to 110.7) and 73.15 mg/L in the D/H@$CaCO_3$ group (95% confidence interval: 47.24 to 127.5). For zebrafish, it was 57.36 mg/L in the Dim group (95% confidence interval: 38.08 to 90.72) and 73.15 mg/L in the D/H@$CaCO_3$ group (95% confidence interval: 81.93 to 122.2). These results indicated that D/H@$CaCO_3$ offers improved biocompatibility and environmental safety.

To examine the distribution of D/H@$CaCO_3$ within the plants, we treated romaine lettuce roots and leaves with FITC-tagged D/H@$CaCO_3$. After exposing the romaine lettuce roots to stained D/H@$CaCO_3$ for 12 h, fluorescence was discernible in both the roots and stems. This indicated that D/H@$CaCO_3$ entered the roots from the water and was subsequently transported to the stems. Upon applying D/H@$CaCO_3$ to romaine lettuce leaves, a distinct green fluorescence was visible within the leaf stomata, highlighting the entry of D/H@$CaCO_3$ through these stomata (Fig. 4g). Additionally, we co-incubated the mycelia of *S. sclerotiorum* with D/H@$CaCO_3$ for 12 h and observed fluorescent signals in the mycelia, suggesting that D/H@$CaCO_3$ was successfully taken up by *S. sclerotiorum* (Fig. S6 in Supporting information).

In this study we formulated a delivery system, D/H@$CaCO_3$, by coating HMSNs with $CaCO_3$ to encapsulate Dim for treating *S. sclerotiorum* in romaine lettuce. The D/H@$CaCO_3$ had a uniform particle size. The $CaCO_3$ on the surface of D/H@$CaCO_3$ functioned as a protective barrier, ensuring the stability of Dim by mitigating leakage, volatilization, and photodegradation. Crucially, in the acidic microenvironment induced by *S. sclerotiorum* on romaine lettuce leaves, $CaCO_3$ is degraded, thereby facilitating the pH-responsive release of Dim to combat the pathogen effectively. This approach demonstrated heightened antifungal efficacy against *S. sclerotiorum* compared with Dim alone, offering extended protection against plant fungal infections. Furthermore, the $CaCO_3$ coating of D/H@$CaCO_3$ upon degradation releases CO_2, increasing the content of pigments such as chlorophyll a, chlorophyll b, and carotenoids for photosynthesis, which is conducive to plant growth. Notably, our findings showed that D/H@$CaCO_3$ could penetrate romaine lettuce roots, get transported to the stems, and enter leaves *via* stomata, underscoring its potential as a carrier for fungicide delivery to plants. Dim as a fungicide has been applied in the plant for inhibiting *S. sclerotiorum* under the good agricultural practice settings dose [28,29]. In addition to the enhanced delivery, SiO_2 has been exploited as Food and Drug Administration (FDA) approved excipient for carrying drugs in oral administration with good characteristics of biological safety and economy [30–33]. Our data from the comprehensive safety evaluations of D/H@$CaCO_3$ revealed that it was nontoxic to seeds, seedlings, earthworms, and zebrafish, emphasizing its potential as a biosafe and environmentally friendly solution for fungicide delivery. These results indicated that the high efficacy of D/H@$CaCO_3$ in inhibiting *S. sclerotiorum*. and turn promoting plant growth could be beneficial to the planting and marketing of lettuce as edible vegetables. This involved HMSNs@$CaCO_3$-based fungicide delivery system with antifungal activity and pH-responsive release could have applications in several protecting crops from pests and plant pathogens, such as HMSNs@$CaCO_3$-based anti-pests and anti-bacteria in modern agriculture.

Declaration of competing interest

The authors declare that they have no known competing financial interests or personal relationships that could have appeared to influence the work reported in this paper.

Acknowledgments

The authors gratefully acknowledge the support of this research by National Key R&D Program of China (No. 2022YFE0139800), National Natural Science Foundation of China (Nos. 82272154, 32201101), the Non-profit Central Research Institute Fund of Chinese Academy of Medical Sciences (No. 2023-JKCS-12), Tianjin Science Fund for Distinguished Young Scholars (No. 22JCJQJC00120), the Fundamental Research Funds for the Central Universities (Nos. 2021-RC310–005, 3332023069), Science and Technology Program of Tianjin City (the Basic Research Cooperation Special Foundation of Beijing-Tianjin-Hebei Region, No. 22JCZXJC00060), the Key Project of Basic Research of Shenzhen (No. JCYJ20200109113603854), Chinese Academy of Medical Sciences Innovation Fund for Medical Sciences (Nos. 2021-I2M-1–058, 2022-I2M-2–003), the Central Government Guides Local Special Funds for Scientific and Technological Development (No. ZY20198002), and Guilin Scientific Research and Technology Development Plan (No. 20210227–3).

Supplementary materials

Supplementary material associated with this article can be found, in the online version, at doi:10.1016/j.cclet.2024.109697.

References

[1] Y.H. Gao, Y.A. Xiao, K.K. Mao, et al., Chem. Eng. J. 383 (2020) 123169.
[2] R. Bagchi, R.E. Gallery, S. Gripenberg, et al., Nature 506 (2014) 85–88.
[3] W.J. Zhang, C.H. Hong, R.Y. Wang, et al., Int. J. Biol. Macromol. 219 (2022) 1112–1121.
[4] C.L. Xu, L.D. Cao, C. Cao, et al., Chem. Eng. J. 452 (2023) 139195.
[5] A. Shelar, S.H. Nile, A.V. Singh, et al., Nano Micro Lett. 15 (2023) 153–189.
[6] K. Wang, Y. Wang, Y.Y. Wu, et al., Chem. Eng. J. 474 (2023) 146012.
[7] M.M. Hossain, F. Sultana, W.Q. Li, L.S.P. Tran, M.G. Mostofa, Cells 12 (2023) 1063.
[8] Z.A. Xie, W.L. Liang, Q.Y. Xiong, et al., Carbohydr. Polym. 291 (2022) 119576.
[9] W. Wei, L.S. Xu, H. Peng, et al., Nat. Commun. 13 (2022) 2213.
[10] C. Zhang, X.M. Wu, Y.Y. Wu, et al., J. Hazard. Mater. 403 (2021) 123888.
[11] L.H. Zheng, J.P. Wu, H. Hu, et al., J. Control. Release 361 (2023) 427–442.
[12] M. Dong, R. Tang, J. Li, et al., Chin. Chem. Lett. 35 (2024) 108539.
[13] J. Wang, H. Pan, J.Y. Li, et al., Chin. Chem. Lett. 34 (2023) 107828.
[14] C. Xu, H.E. Dobson, M.J. Yu, et al., J. Control. Release 357 (2023) 84–93.
[15] L.J. Ju, Z.X. Huang, Q. Shen, et al., Chin. Chem. Lett. 35 (2024) 109450.
[16] R. Tan, X.Y. Qiu, W.Y. Mu, et al., Chin. Chem. Lett. 35 (2024) 108343.
[17] W.C. Li, H.J. Zhou, X.Y. Zhang, et al., ACS Nano 17 (2023) 15199–15215.
[18] Y. Ding, Z.G. Xiao, F.R. Chen, et al., Sci. Total Environ. 863 (2023) 160900.
[19] Z.Q. Shi, Q.Q. Li, L. Mei, Chin. Chem. Lett. 31 (2020) 1345–1356.
[20] Y.H. Gao, Y.H. Zhang, S. He, et al., Chem. Eng. J. 364 (2019) 361–369.
[21] C.L. Xu, Y.P. Shan, M. Bilal, et al., Chem. Eng. J. 395 (2020) 125093.
[22] Y.H. Gao, Y. Liang, H.Q. Dong, et al., ACS Sustain. Chem. Eng. 8 (2020) 5716–5723.
[23] P. Huang, D.Z. Lian, H.L. Ma, et al., Chin. Chem. Lett. 32 (2021) 3696–3704.
[24] X.D. Yang, S.M. Ying, S. Zhang, et al., Chin. Chem. Lett. 35 (2024) 108674.
[25] S.J. Song, Y.L. Wang, J. Xie, et al., ACS Appl. Mater. Interfaces 11 (2019) 34258–34267.
[26] L. Boufeldja, F. Boudard, K. Portet, et al., Int. J. Mol. Sci. 24 (2023) 12815.
[27] L. Loladze, J.M. Nolan, L.H. Ziska, A.R. Knobbe, Mol. Nutr. Food Res. 63 (2019) 1801047.
[28] J.Y. Tang, G. Tang, J.F. Niu, et al., J. Agric. Food Chem. 69 (2021) 2382–2391.
[29] Y.X. Gao, X. Zhang, X.N. Song, et al., Pest Manage. Sci. 80 (2024) 1981–1990.
[30] Q.Q. Li, Z.Q. Shi, M.T. Ou, et al., J. Control. Release 352 (2022) 450–458.
[31] R. Mohammadpour, D.L. Cheney, J.W. Grunberger, et al., J. Control. Release 324 (2020) 471–481.
[32] Y.X. Wang, L. Zhao, Y.B. Dai, et al., Adv. Mater. 35 (2023) 2307900.
[33] Y.D. Deng, X.D. Zhang, X.S. Yang, et al., J. Hazard. Mater. 409 (2021) 124502.